Bioorganic Chemistry 169 (2026) 109452

Contents lists available at ScienceDirect

Bioorganic Chemistry

journal homepage: www.elsevier.com/locate/bioorg

Natural products as payloads for antibody-drug conjugates: Cyclopamine linked to cetuximab for hedgehog pathway inhibition

Giovanni Ricciardella [a,1], Francesca Migliorini [a,1], Luisa Maresca [b,c,1], Elena Cini [a], Giovanni Ievoli [a], Elena Petricci [a,**], Maurizio Taddei [a,*], Demetra Zambardino [a], Barbara Stecca [b], Alberto Montalbano [d], Enrica Crivaro [b]

[a] Dipartimento di Biotecnologie, Chimica e Farmacia, Università di Siena, Via A. Moro 2, 53100 Siena, Italy
[b] Core Research Laboratory - Istituto per lo Studio, la Prevenzione e la Rete Oncologica (ISPRO), Viale Pieraccini 6, 50139 Firenze, Italy
[c] Department of Experimental and Clinical Biomedical Sciences "Mario Serio", University of Florence, Italy
[d] Dipartimento di Medicina Sperimentale e Clinica (DMSC), Università di Firenze, Viale Pieraccini 6, 50139 Firenze, Italy

ARTICLE INFO

Keywords:
Antibody-drug conjugate
Natural products
Hedgehog signalling pathway
Click chemistry

ABSTRACT

Cyclopamine, a natural product that enabled the identification of Smoothened as a central regulator of the Hedgehog (HH) signalling pathway, has never advanced to clinical testing due to unfavourable pharmacokinetics and multiple off-target effects. In this study, we describe two novel antibody-drug conjugates (ADCs) in which Cetuximab is covalently linked to cyclopamine, to selectively deliver this natural product into melanoma cells exhibiting HH pathway activation and epidermal growth factor receptor (EGFR) expression. The ADC, which contains an acid-cleavable linker, effectively inhibited GLI1 and GLI2 expression and demonstrated anti-proliferative activity in melanoma cell lines A375 and SK-MEL-5, highlighting the efficacy of cyclopamine and monoclonal antibody (mAb) conjugation. This activity was associated with a pro-apoptotic effect directly linked to HH pathway inhibition. The linker-payload system was stable in plasma yet released gradually cyclopamine at pH 5.5. These results suggest the feasibility of using natural products as payloads for the construction of ADCs to inhibit HH signalling in cancer cells.

1. Introduction

Cyclopamine is a natural alkaloid extracted from *Veratrum californicum*, a lily of the *Melanthiaceae* family native to the northern hemisphere, particularly the mountainous regions of the western United States [1]. The observation that lambs born to sheep fed on *Veratrum californicum* showed severe craniofacial defects resembling the phenotype of mice lacking *Shh* [2,3], suggested that cyclopamine itself suppresses the Hedgehog (HH) signalling. HH signalling plays a central role in regulating embryonic development, tissue homeostasis, and cell proliferation and differentiation [4]. Abnormal activation of the HH signalling pathway is involved in several types of cancer, including those of the skin [5]. Canonical activation of the HH signalling is initiated by the binding of HH ligands to the transmembrane receptor Patched 1 (PTCH1), which releases the inhibition on the G protein-coupled receptor Smoothened (SMO). Active SMO triggers an intracellular cascade that ultimately leads to the activation and nuclear translocation of the GLI transcription factors [5]. Cyclopamine was found to inhibit HH signalling, by directly binding SMO [6,7]. However, this molecule has never reached the clinical phase of drug development due to poor solubility [8], gastric instability and adverse side effects observed in animal model [9]. The more active and metabolically stable derivative IPI-926 [10], also known as saridegib, reached phase 3 clinical trials for the treatment of basal cell carcinoma in patients with Gorlin syndrome, and other clinical trials are still ongoing [11]. Only the SMO inhibitors vismodegib [12], sonidegib [12] and glasdegib [13] have been approved by the FDA to date (Chart 1).

ADCs are characterized by high target specificity and binding affinity, good stability in the bloodstream and internalisation efficiency, demonstrating their superior efficacy compared to standard

* Corresponding author.
** Corresponding author.
E-mail addresses: elena.petricci@unisi.it (E. Petricci), maurizio.taddei@unisi.it (M. Taddei).
[1] These authors contributed equally to the work.

https://doi.org/10.1016/j.bioorg.2025.109452
Received 15 September 2025; Received in revised form 13 December 2025; Accepted 27 December 2025
Available online 31 December 2025

chemotherapies. [14] Since 2000, regulatory agencies have approved more than 15 ADCs for the treatment of cancer. [15] Most of them are loaded with highly cytotoxic payloads as tubulin inhibitors, DNA alkylating agents or potent inducers of DNA double-strand breaks [16]. Since diversifying the mechanism of the therapeutic molecule is crucial for the success of cancer treatments [17] we have recently investigated the activity of ADCs with unconventional payloads as HDAC inhibitors [18–21]. Inspired by the great interest in cyclopamine due to its particular history and chemical structure [22,23], we decided to investigate whether the incorporation of this natural product into an ADC system could enhance its anticancer activity, with the aim of circumventing some of the pharmacokinetic limitations observed to date. Cyclopamine is available as a natural product extracted from vegetable sources [24] and biotechnological production of cyclopamine is feasible and progressing rapidly [25,26]. Recently, a divergent and scalable syntheses of cyclopamine has been reported starting from inexpensive dehydro-epi-androsterone [27].

2. Results and discussion

For the conjugation of cyclopamine with an antibody, we designed a non-cleavable linker based on a 3-thio-maleimide core for standard release of the drug after internalisation and lysosomal metabolism [18] and the acid-labile linker 5-(hydroxymethyl)pyrogallol orthoester (HMPO) [28], which can release the drug in the acidic lysosomal space (pH 4.5–5.5). Michael reaction of propargyl maleimido compound **2** with freshly prepared *p*-mercaptobenzyl alcohol gave the compact linker **3** characterized by a benzyl alcohol for the attachment of the alkaloid and an alkyne for click chemistry to introduce the spacer for the link of the antibody (Scheme 1). Activation of **3** with *p*-nitrophenylchloroformate followed by addition of cyclopamine **1** gave compound **4** in 76 % yield over two steps. The Cu-catalysed Huisgen reaction with 6-azidohexanoic acid (**5**) yielded compound **6**, a molecule in which the carboxylic acid is the future coupling point for the antibody lysines. Alternatively, we prepared the acid-cleavable linker **7** derived from gallic acid and, after activation *p*-nitrophenylchloroformate, addition of cyclopamine **1** gave compound **8**, further converted to acid **9** via a Cu-catalysed Huisgen reaction with azide **5** (Scheme 1).

Based on our experience on ADC preparation [18], we selected Cetuximab (Ctx), a commercially available mAb directed towards epidermal growth factor receptor (EGFR). A first attempt to bioconjugate compounds **6** and **9** with Ctx via in situ activation with water-soluble sulfo-NHS (**10**) in DMSO/EPPS followed by addition of a freshly prepared stock solution of Cetuximab (Ctx) in EPPS at pH ≈ 8.0 gave positive results only with **9** that was linked to Ctx (**ADC-11** in Scheme 2A) with a Drug-Antibody Ratio (DAR) = 1.90 (MALDI analysis, see SI). Attempts to prepare the activate N-hydroxysuccinimide of **6** and use it for bioconjugation with Ctx were unsuccessful. Thus, we decided to carry out a biorthogonal click reaction to attach the uncleavable linker to Ctx. The NHS activated carboxylate **12** reacted with dibenzylcyclooctyne amine **13** to give amide **14** in 58 % isolated yield Scheme 2 B). In parallel, Ctx was incubated with the NHS ester of 14-azido-3,6,9,12-tetraoxatetradecanoic acid (**15**) to give azido pre-functionalized Ctx (**Ctx—N_3**) with a DAR = 1.78 (MALDI analysis, see SI). Further reaction of **Ctx-N_3** in PBS with a DMSO solution of amide **9** gave the expected **ADC-16** charged with cyclopamine with a DAR = 1.02 (Scheme 2B).

The different behaviour during bioconjugation could be related to the different lipophilicity of the linker-payload systems, as previously reported [29].

Biological activity of **ADC-11** and **ADC-16** was evaluated on melanoma cell lines. Melanoma is an aggressive form of skin cancer, characterized by high heterogeneity and metastatic potential. Melanomas display aberrant HH pathway activation, as demonstrated by the higher expression of SMO, GLI1, GLI2 and PTCH1, compared with normal melanocytes [30,31]. In order to select the most suitable melanoma cell line for the biological characterisation of ADCs, the expression levels of EGFR, the target of cetuximab, and of GLI1 and GLI2, the final effectors of the HH pathway, were investigated in five melanoma cell lines by Western blot. Melanoma cell lines A375 and SK-MEL-5 showed the higher expression of EGFR and of either GLI1 or GLI2 and were used for the subsequent ADCs evaluation. The breast cancer T-47D cells, which express EGFR and GLI1, was used as a positive control (SI Fig. S2).

The antiproliferative activity of Cetuximab, cyclopamine (**1**), ADCs (**11** and **16**), and unconjugated linker-payload (**6** and **9**) was investigated. Both melanoma cell lines were treated at two concentrations (100 μg/mL-200 μg/mL) [28] for 72 h. ADCs **11** and **16** reduced melanoma cells viability, while the single components Ctx, **1** and unconjugated **9** and **6** had no effect compared to untreated cells (NT) (Fig. 1A and B). ADCs **11** and, to a lesser extent, ADC **16** inhibited EGFR and HH signalling, as shown by the reduced levels of pEGFR (Tyr11739) and pERK1/2, targets of the EGFR cascade, and of GLI1 and GLI2 in A375 cells (Fig. 1C).

As compound **11** was more effective in suppressing the EGFR cascade and in reducing the expression of GLI2 and GLI1, we selected ADC **11** for further biological characterisation. Full concentration dose-response curves and IC50 values were obtained for Cetuximab, **1**, unconjugated **9** and ADC **11** in A375 and SK-MEL-5 melanoma cells. Importantly, IC50 values of ADC **11** were lower than cyclopamine (**1**), Cetuximab, and unconjugated **9** (Fig. 1D-F). Western blot analysis further confirmed that ADC **11** inhibited the expression of pEGFR and the downstream targets

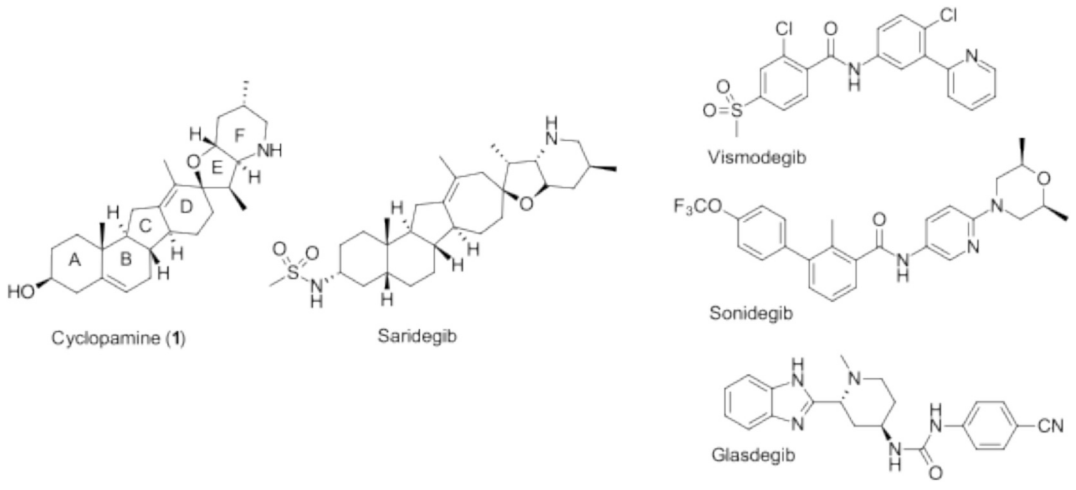

Chart 1. Structures of cyclopamine, saridegib and the three FDA-approved Smoothened inhibitors.

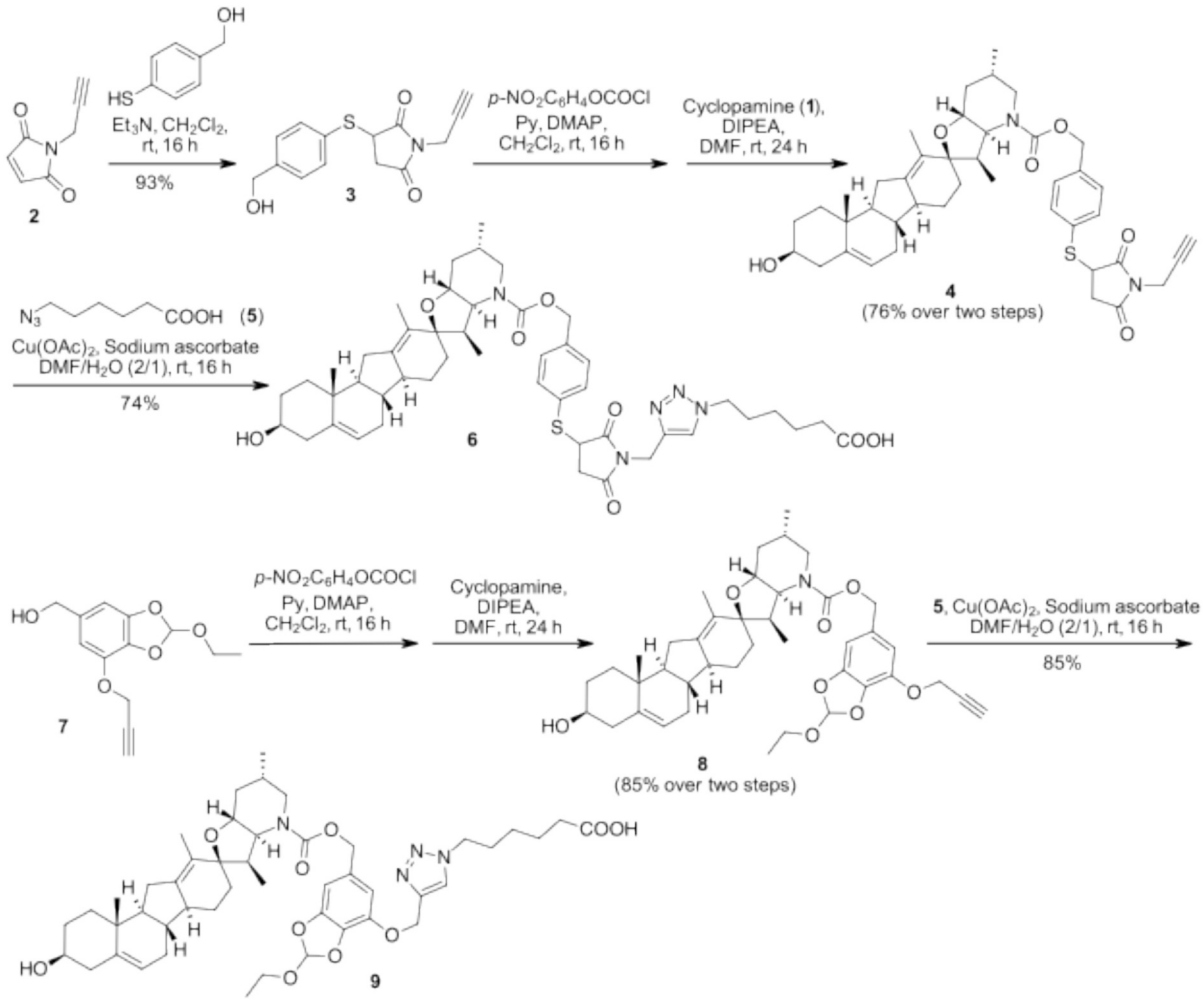

Scheme 1. Preparation of the linkers carrying cyclopamine (**1**) for the conjugation with the antibody lysines.

(p-ERK1/2 and p-AKT) in both A375 and SK-MEL5 cell lines. Moreover, ADC **11** reduced the expression of GLI2 in A375 cells and of both GLI1 and GLI2 in SK-MEL-5 cells (Fig. 3G). On the other hand, treatment with Ctx or cyclopamine alone had no effect on the protein levels of the selected targets, confirming the efficacy and specificity of ADC. In addition, unconjugated **9** did not exert an inhibitory effect on EGFR signalling cascade (Fig. S3). Furthermore, the ADC **11** demonstrated greater efficacy in reducing melanoma cell viability than the combination of unconjugated Ctx and cyclopamine, indicating that its antiproliferative activity arises from EGFR-mediated delivery of cyclopamine to melanoma cells (see SI, Fig. S4). To understand whether the antiproliferative effect is due to a reduction in proliferation or an increase in cell death, we first assessed the cell cycle distribution using propidium iodide staining of A375 and SK-MEL-5 cells. Treatment of melanoma cells with Ctx, cyclopamine (**1**) and **11** for 72 h did not affect cell cycle in either melanoma cell line, as the cells distribution did not change at the different stages of the cell cycle (G0/G1, S, M) (Fig. 2A-D). Consistently, the expression of of PCNA, a marker of G1/S transition, was not changed in both melanoma cell lines (Fig. 2E).

To assess whether the observed antiproliferative effect is due to an increase in apoptosis, we performed AnnexinV/7-AAD staining followed by flow cytometry. Treatment of A375 and SK-MEL-5 cells with **11** resulted in an increase of early and late apoptosis in SK-MEL-5, whereas only early apoptosis was affected in A375 cells (Fig. 3A and B and S5). Ctx, cyclopamine and **9** did not significantly affect apoptosis. The pro-apoptotic effect of ADC **11** was further confirmed by the reduced expression of anti-apoptotic marker BCL2, and by the increase of pro-apoptotic markers BAX and cleaved caspases 3 and 9 (Fig. 3C).

Finally, cell internalisation of **11** was investigated using the Fabfluor-pH Red Antibody Labelling Dye, which releases a red fluorescent signal when the Fab-Ab complex is internalized and processed in lysosomes (pH 4.5–5.5). Cetuximab, ADC **11** and culture medium (negative control) were incubated with IncuCyte® Human FabFluor-pH Red Antibody Reagent according to the manufacturer's protocol [32]. After 48 h, a red fluorescence signal was observed in live melanoma cells treated with Ctx or ADC **11,** but not in cells treated with culture medium (see SI, Fig. S6), confirming the interaction of ADC **11** with EGFR and further internalisation for the release of cyclopamine.

Since our most promising ADCs is based on a pH-sensitive linker, we determined the behaviour of **9** in plasma, PBS and at pH 5.5. The unconjugated molecule was relatively stable in plasma and PBS at pH 7.4 ($t_{1/2}$ > 48 h in both cases, Fig. 4A) and slowly released cyclopamine at pH 5.5 (Fig. 4B). As cyclopamine **1** has been reported to be unstable in an acidic environment [33] we determined also the stability of **1** at pH 5.5 comparing with its behaviour in water and at pH 2.0 as a positive control. While a peak related to a degradation product (about 40 %) appears in the HPLC trace after 12 h at a pH of 2.0, cyclopamine is stable up to 48 h after incubation in water and at a pH of 5.5 (Fig. 4C and Fig. S11). These data confirm that cyclopamine is stable under the conditions in which it is expected to be released from the ADC

3. Conclusions

In summary, with this work we have shown the feasibility of using

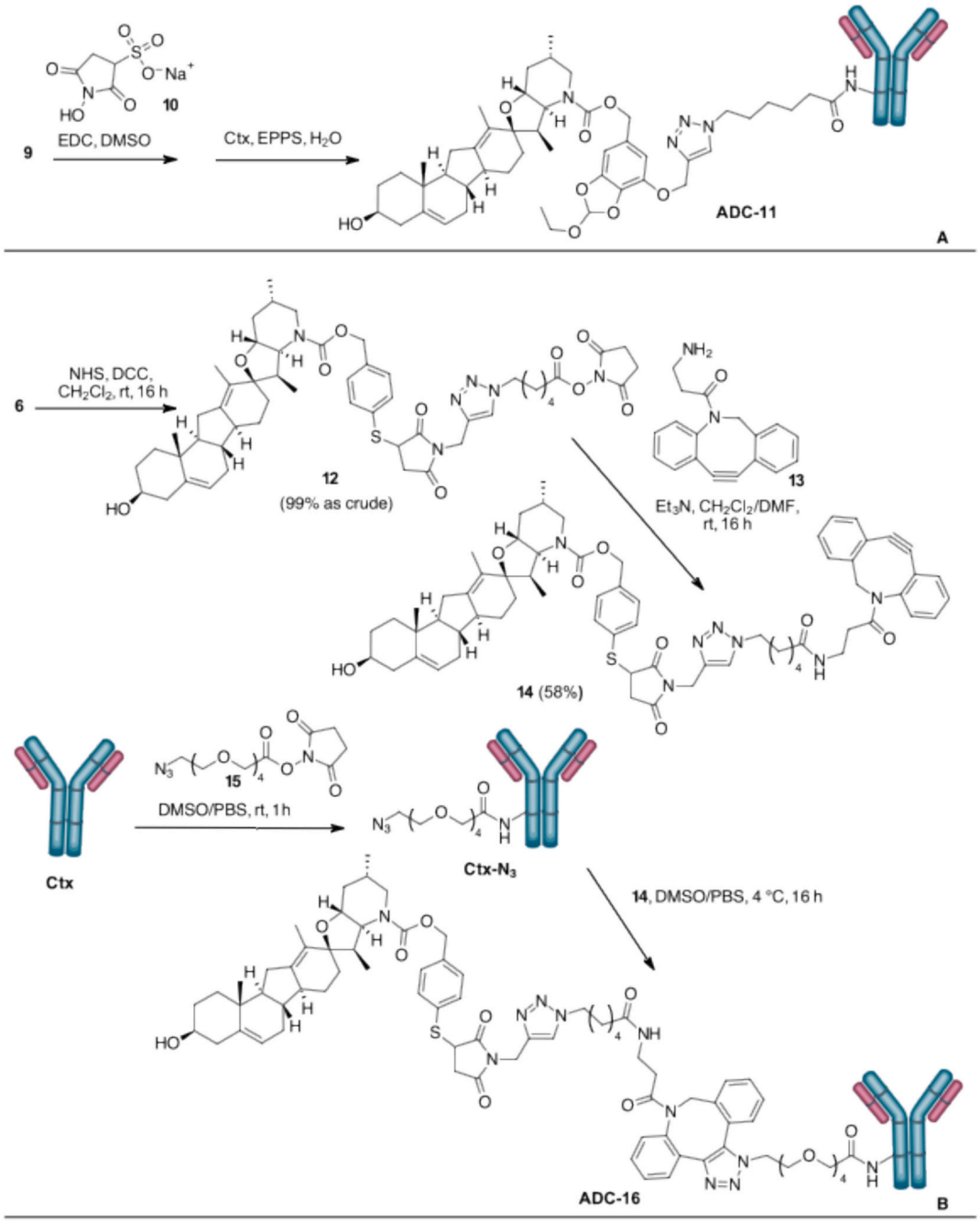

Scheme 2. Bioconjugation of linkers **9** and **6** with Cetuximab.

natural products that are not particularly cytotoxic, such as cyclopamine, for the construction of an ADC that can deliver cyclopamine into cancer cells expressing EGFR. This bioconjugate combines the selectivity of Ctx with the antiproliferative activity of cyclopamine. In two melanoma cell lines, this ADC impairs cell viability through a strong pro-apoptotic effect more effectively than Ctx or cyclopamine alone. ADC **11** also suppresses the HH and EGFR cascades with inhibition of GLI1 and GLI2 expression, while Ctx and cyclopamine alone or in combination did not achieve the same level of efficacy. Building on these encouraging results, we are exploring bioconjugation via antibody cysteines using alternative inhibitors of the HH signalling pathway as payloads for future in vivo studies.

4. Experimental section

4.1. General methods

All reagents were purchased from commercial suppliers and used without further purification. The reactions were carried out in oven dried or flamed vessels. Solvents were dried and purified by conventional methods [34] prior use or, if available, purchased in anhydrous form. Flash column chromatography was performed with Merck silica gel 60, 0.040–0.063 mm (230–400 mesh). Merck aluminum backed plates pre-coated with silica gel 60 (UV 254) were used for analytical thin layer chromatography and were visualized by staining with a $KMnO_4$ solution. NMR spectra were recorded at 25 °C and 400 or 600 MHz for ^{1}H and 100 or 150 MHz for ^{13}C. The solvent is specified for each spectrum. Splitting patterns are designated as s, singlet; d, doublet; t,

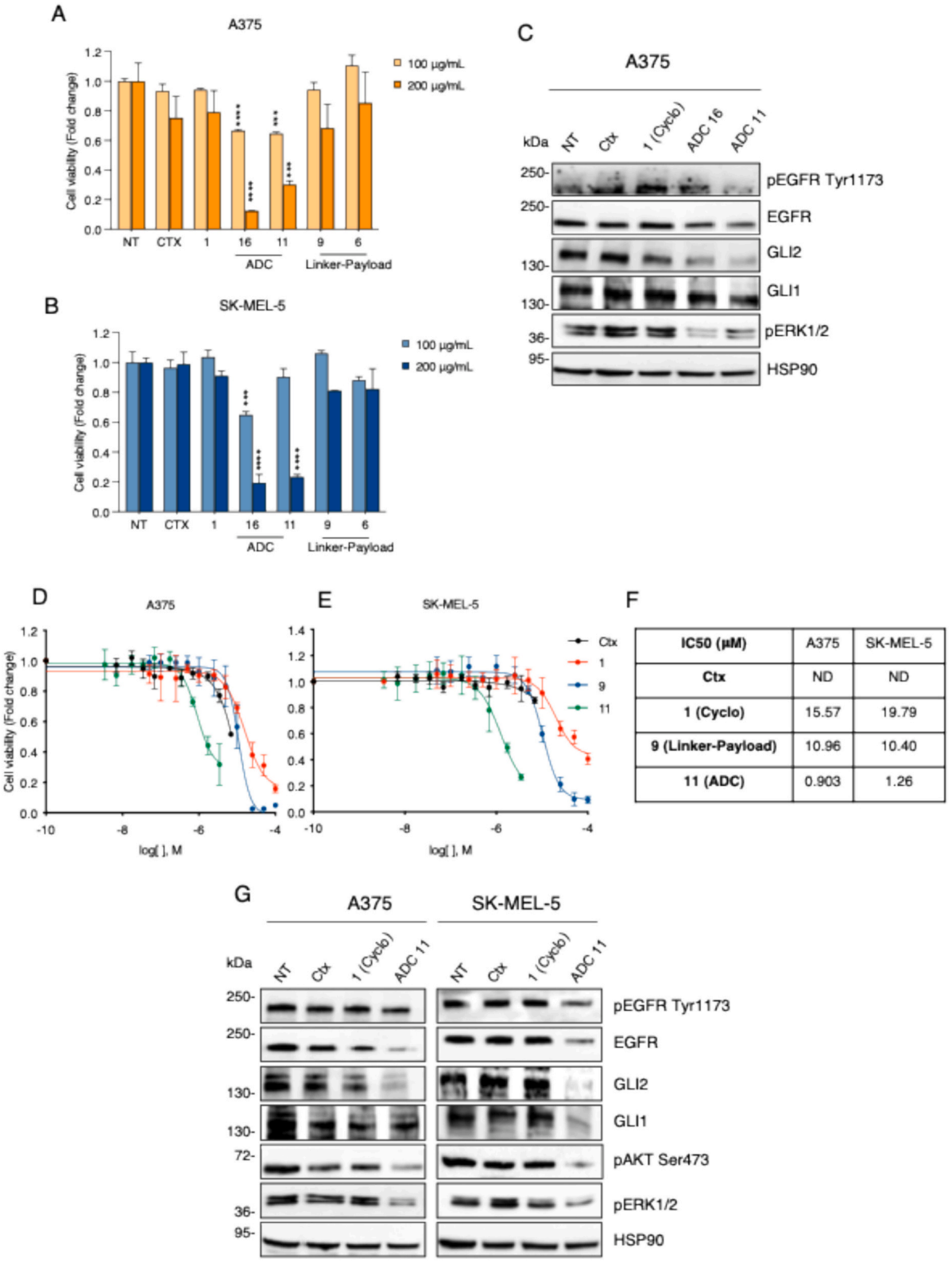

IC50 (µM)	A375	SK-MEL-5
Ctx	ND	ND
1 (Cyclo)	15.57	19.79
9 (Linker-Payload)	10.96	10.40
11 (ADC)	0.903	1.26

Fig. 1. ADCs reduce melanoma cell viability and inhibit EGFR and HH signalling. **A,B)** Cell viability analysis in A375 (A) and SK-MEL-5 (B) melanoma cells treated for 72 h with Cetuximab (Ctx), cyclopamine (**1**) ADCs **11** and **16** and unconjugated payloads **9** and **6**. Untreated cells (NT) were used as control and equated to 1. **C**) Western blot analysis of pEGFR, EGFR, pERK1/2, GLI1 and GLI2 proteins in A375 melanoma cells treated with Cetuximab (Ctx), cyclopamine (**1**) ADCs **11** and **16** at 200 µg/mL for 72 h. HSP90 was used as loading control. **D,E)** Dose-response curves of Cetuximab (Ctx), cyclopamine (**1**) ADC **11**, and unconjugated payload **9** in A375 (D) and SK-MEL-5 (E) melanoma cells. **F)** IC50 values of Cetuximab (Ctx), cyclopamine (**1**) ADCs **11** and **16** and unconjugated payloads **9**. **G**) Western blot analysis of pEGFR, EGFR, pAKT, pERK1/2, GLI1 and GLI2 in A375 and SK-MEL-5 treated as indicated for 72 h. NT, untreated cells. Data represent mean ± SD of at least three independent experiments. ***, $p < 0.001$; ****, $p < 0.0001$ (one-way ANOVA).

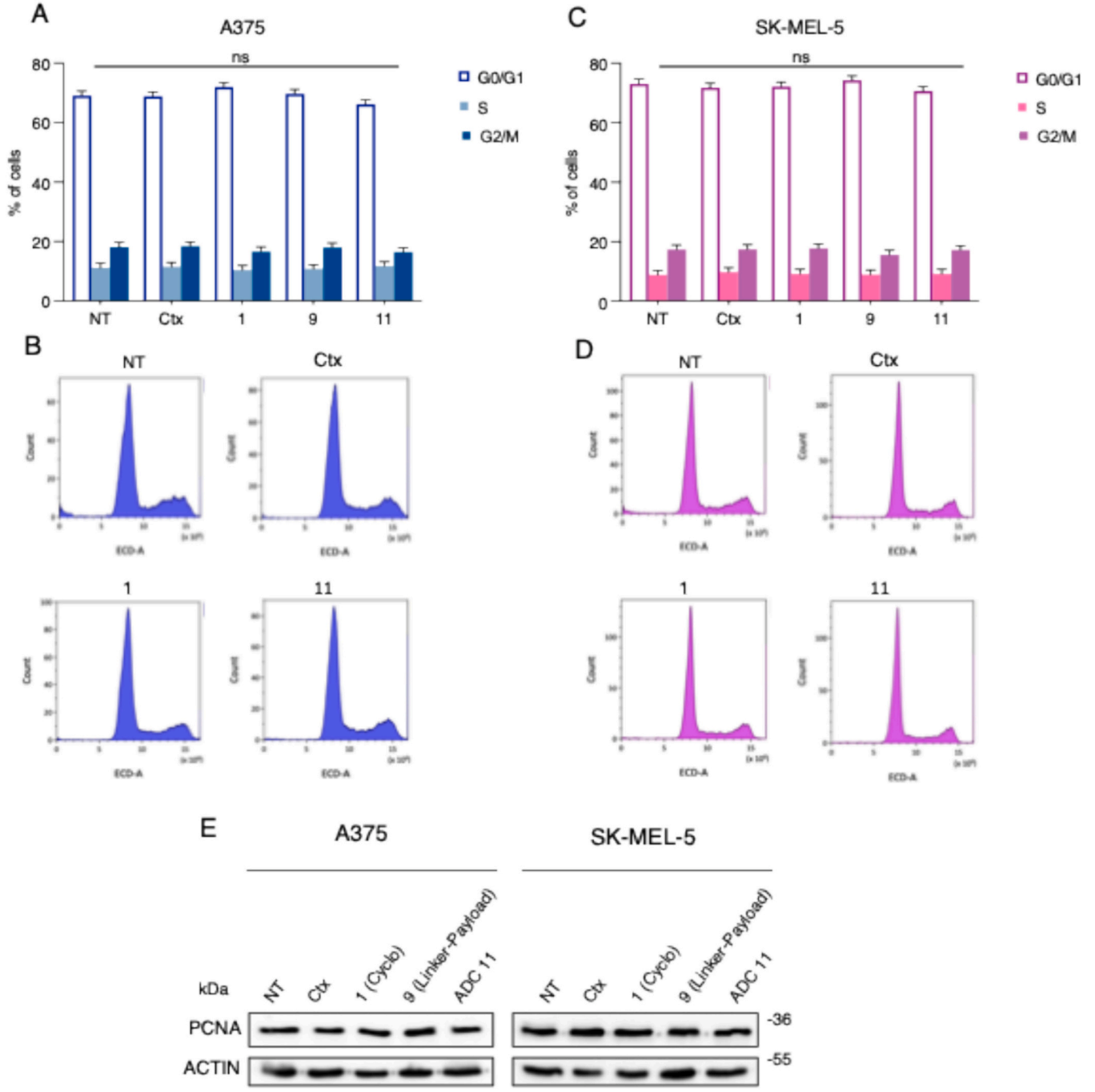

Fig. 2. ADC 11 does not affect cell cycle distribution in melanoma cells. FACS analysis of cell cycle distribution in A375 (**A,B**) and SK-MEL-5 **(C,D)** treated for 72 h with Cetuximab, **1** and ADC **11** at 200 μg/mL. Representative cell distribution plots in different phases of the cell cycle in A375 (**B**) and SK-MEL-5 (**D**) cell lines. **E)** Western blot of PCNA in A375 and SK-MEL-5 cells treated as indicated for 72 h. ACTIN was used as loading control. NT, untreated cells. All ns: not significant (one-way ANOVA). Data represent mean ± SD of at least three independent experiments.

triplet; q, quartet; m, multiplet; br, broad. Chemical shifts (d) are given in ppm relative to the resonance of their respective residual solvent peaks. High-resolution mass spectroscopy analyses were recorded by electrospray ionization with a mass spectrometer Q-exactive Plus. Low resolution MS and HPLC/MS analysis were performed with the chromatographic LC/MSD system Agilent 1260 Infinity II, connected with UV detector (254 nm) using an Phenomenex Kinetex® EVO C18 column (2.6 μm), flow 0.6 mL/min, MeCN (0.1 % HCOOH)/H_2O (0.1 % HCOOH) gradient from 5:95 to 95:5 in 10 min or 5:80; 80:95 to 95:5 in 10 min. ESI ionization, flow of the drying gas (N_2) 9 L/min, temperature 330 °C, atomizing pressure 40 PSI, fragmentation 135 eV. HRSMS analysis were done using a Bruker Elute HPLC with autosampler and UV-DAD, coupled with a Bruker TimsTOF spectrometer and API source. LC analyses of plasma stability tests were performed by using Agilent 1260 L. MSD single-quadrupole instrument was equipped with the orthogonal spray API-ES (Agilent Technologies, Palo Alto, CA). The pressure of the nebulizing gas and the flow of the drying gas (nitrogen used for both) were set at 40 psi and 9 L/min, respectively. The capillary voltage, the fragmentor voltage, and the vaporization temperature were 3000 V, 10 V, and 350 °C, respectively. MSD was used in the positive and negative ion mode. Spectra were acquired over the scan range m/z 100–1500 using a step size of 0.1. Chromatographic analyses were performed using

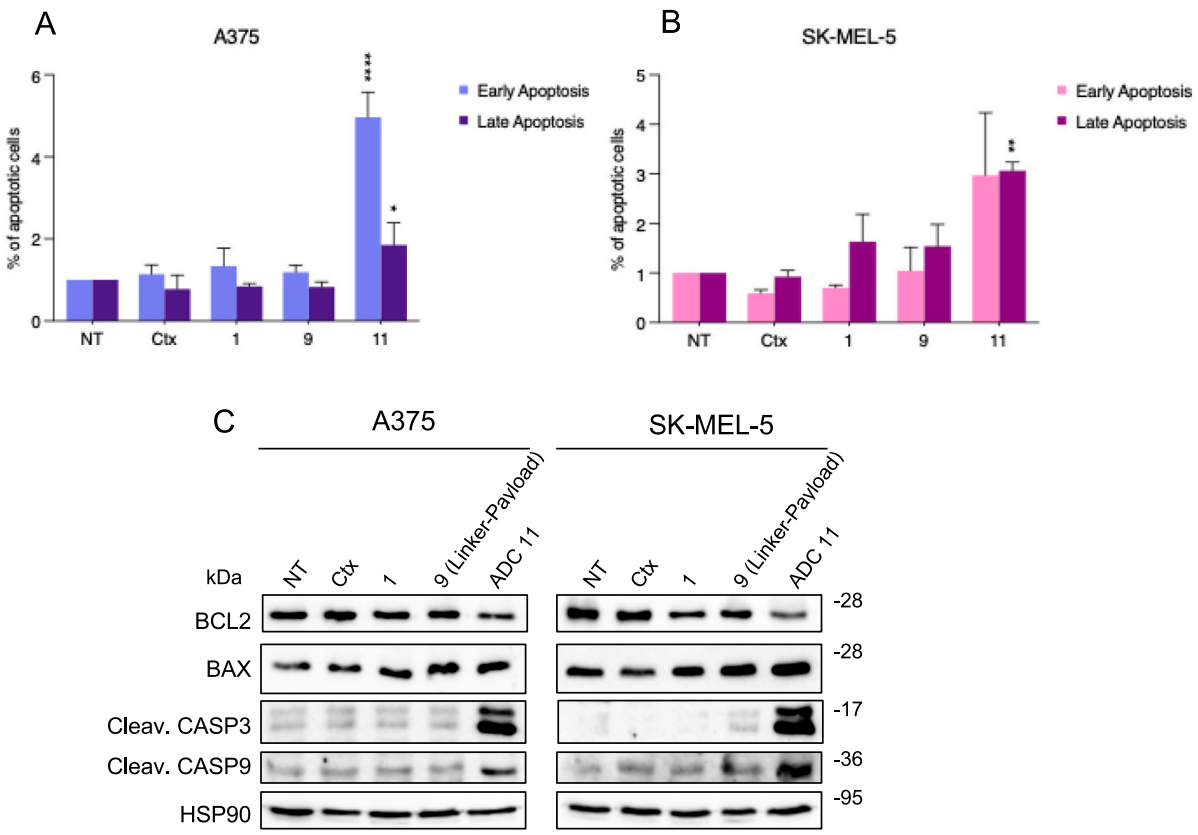

Fig. 3. ADC 11 treatment increases apoptosis in melanoma cells. A,B) Analysis of early and late apoptosis in A375 (A) and SK-MEL-5 (B) cells after treatment with Ctx, Cyclopamine (**1**), **9** (linker-payload unit) and ADC **11** for 72 h; Untreated cells (NT) were used as control and equated to 1. Examples of cytofluorimetric plots following double staining Annexin V/7-AAD are reported in SI. **C)** Western blot of BCL2, BAX, cleaved caspases 3 and 9 in melanoma cells treated as indicated. HSP90 was used as loading control. *$p < 0.05$; **$p < 0.01$; ****$p < 0.0001$. Data represent mean ± SD of at least three independent experiments.

a Phenomenex Kinetex EVO C18-100 Å (100 × 4.6 mm, 2.6 µm particle size) at room temperature, at flow rate of 0.6 mL/min, and injection volume of 5 µL, operating with a gradient elution of A: water (H_2O) and B: acetonitrile (MeCN). Both solvents were acidified with 0.1 % *v*/v of formic acid. UV detection was monitored at 254 and 210 nm. The analysis started with 5 % of B, then B was increased to 80 % in 10 min, then kept at 95 % in 5 min and finally return to 5 % of eluent B in 5.0 min. N-Propargyl maleimide [35] and benzyl alcohol **7** [28] were prepared as previously described.

Human melanoma cell lines A375, MeWo, SK-MEL-2, and SK-MEL-28 cells were obtained from ATCC (Manassas, VA, USA). SK-MEL-5 cell line was kindly provided by Dr. Laura Poliseno (CRL-ISPRO, Pisa, Italy). T-47D breast cancer cell line was kindly provided by Mario Negri Institute (Milano). Cells were cultured in Dulbecco's modified Eagle's medium (DMEM) (Euroclone, Milan, Italy) with 10 % fetal bovine serum (FBS), 1 % Penicillin-Streptomycin, and 1 % Glutamine (Lonza, Basel, Switzerland). Breast cancer cell line T-47D was cultured in RPMI-1640 Medium (Euroclone) supplemented with 10 % FBS (Fetal Bovine Serum, Carlo Erba), 1 % L-Glutammine (Euroclone) and 1 % Penicillin-Streptomycin solution (Euroclone). All cells were maintained in incubator at 37 °C with 5 % CO_2. Mycoplasma was periodically tested by PCR upon thawing of a new batch of cells and cultures were renewed every month. *Statistical analysis:* data represent mean ± SD calculated on at least three independent experiments. Statistical significance was assessed by ANOVA tests for multiple comparisons. P. value <0.05 is considered statistically significant.

3-((4-(Hydroxymethyl)phenyl)thio)-1-(prop-2-yn-1-yl)pyrrolidine-2,5-dione (3)

Under N_2, 4-mercaptobenzoic acid (1.00 g, 6.49 mmol) was solubilised in dry THF (20 mL) and cooled at 0 °C. $LiAlH_4$ 1 M in THF (19.5 mL, 19.5 mmol) was added dropwise and then the reaction mixture was stirred at room temperature for 16 h. The reaction was quenched with HCl 1 N at 0 °C until pH 2.0 and extracted with EtOAc (20 mL × 3). The organic phase was washed with water (20 mL × 2) and brine (20 mL) and dried over dry Na_2SO_4, filtered and evaporated under reduced pressure. The compound was purified by chromatography on silica gel with MPLC Isolera Biotage system eluting 0–30 % gradient of EtOAc in petroleum ether (40–60) giving **2** as a white solid (890 mg, 6.36 mmol, 98 %). Under N_2, 4-mercaptobenzyl alcohol **2** (610 mg, 4.36 mmol) was solubilised in CH_2Cl_2 (20 mL) and triethylamine (30 mL, 0.22 mmol) was added dropwise at 0 °C and the solution stirred at rt. for 30 min. *N*-Propargyl maleimide (1.00 g, 7.41 mmol) was added at 0 °C and the solution stirred at room temperature for 16 h. Triethylamine and CH_2Cl_2 was evaporated under reduced pressure and compound **3** purified by chromatography on silica gel with MPLC Isolera Biotage system eluting with 0–15 % gradient of EtOAc in CH_2Cl_2, as a white solid (1.11 g, 4.05 mmol, 93 % of yield). ^{1}H NMR (600 MHz, $CDCl_3$, δ ppm, *J* Hz) δ 7.54–7.51 (m, 2H), 7.38–7.34 (m, 2H), 4.72 (d, $J = 4.0$ Hz, 2H), 4.20 (d, $J = 2.4$ Hz, 2H), 4.05 (dd, $J = 9.2$, 4.1 Hz, 1H), 3.19 (dd, $J = 9.2$, 5.5 Hz, 1H), 2.73 (dd, $J = 18.8$, 3.7 Hz, 1H), 2.21 (t, $J = 6.0$ 1H). ^{13}C NMR (151 MHz, $CDCl_3$, δ ppm) δ 142.45, 134.76, 128.98, 127.76, 76.03, 71.74, 64.54, 43.95, 35.90, 28.12. ESI: *m/z* 276 $[M + H]^+$.

General procedure for the synthesis of carbamates. Compound 4. The linker **3** (110 mg, 0.40 mmol) was solubilised in dry THF (5 mL) at rt. under N_2. At 0 °C, *p*-nitrophenyl chloroformate (161 mg, 0.80 mmol), DMAP (24 mg, 0.2 mmol) and pyridine (65 mL, 0.80 mmol) were added, and the reaction was stirred for 16 h at room temperature. The formation of the activated compound was checked by TLC and ESI-MS. The THF was evaporated, and the mixture was quickly filtrated on a pad of silica gel using petroleum ether: EtOAc 7:3. The solution was

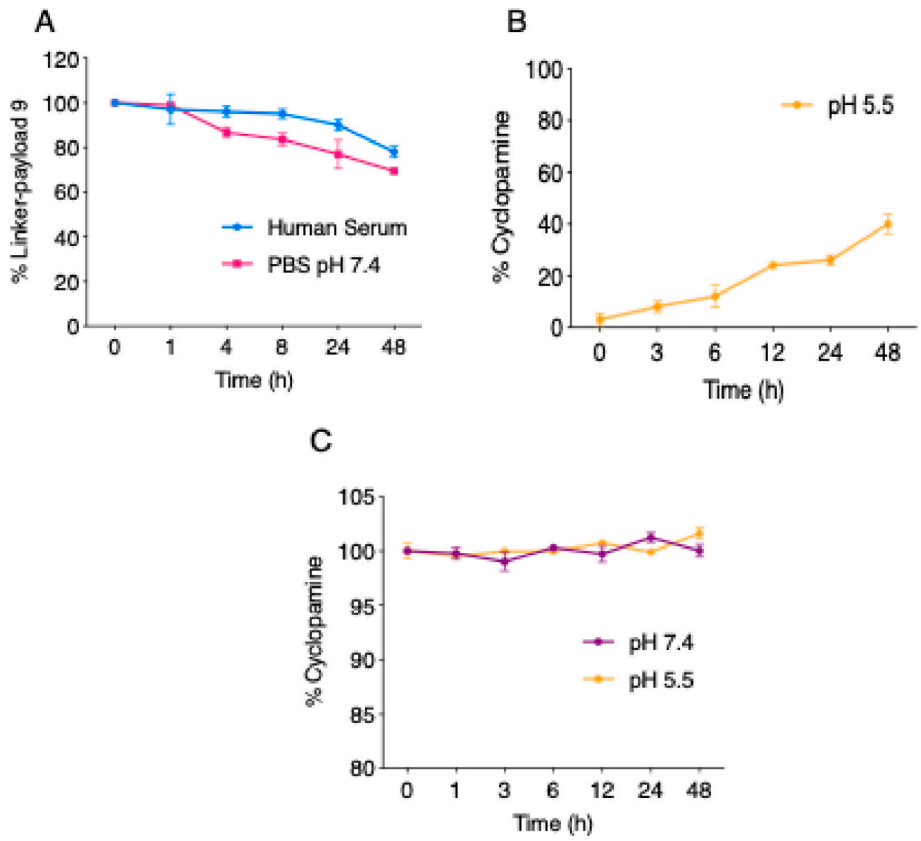

Fig. 4. **A)** HPLC-MS stability of linker-payload system **9** in male human serum or PBS (pH 7.4). **B)** Release of cyclopamine at pH 5.5. **C)** Stability of cyclopamine at pH 5.5 and 7.4.

concentrated under reduced pressure and immediately used in the next step. The residue was solubilised in dry DMF at 0 °C and Cyclopamine (**1**) (0.8 mmol) and DIPEA (418 μL, 2.4 mmol) were added and the reaction stirred at room temperature for 16 h. The solvent was evaporated under reduced pressure with addition of heptane. Compound **4** was purified by chromatography on silica gel with MPLC Isolera Biotage eluting with a gradient of MeOH in CH_2Cl_2 0–5 % and recovered as a white solid (0.216 g, 76 % of yield). ^{1}H NMR (400 MHz, $CDCl_3$, δ ppm, J Hz) 7.50 (d, J = 8.2 Hz, 2H), 7.30 (d, J = 8.0 Hz, 2H), 5.35 (d, J = 2.0 Hz, 1H), 5.10 (s, 2H), 4.16 (dd, J = 2.5, 0.6 Hz, 2H), 4.03 (dd, J = 9.5, 3.8 Hz, 1H), 3.62 (dd, J = 13.0, 4.1 Hz, 1H), 3.55–3.49 (m, 2H), 3.26 (t, J = 6.9 Hz, 1H), 3.20–3.13 (m, 2H), 2.93–2.82 (m, 2H), 2.73–2.66 (m, 2H), 2.34 (s, 1H), 2.22–2.19 (m, 3H), 2.18–2.16 (m, 2H), 1.87–1.79 (m, 3H), 1.67 (s, 2H), 1.64 (s, 3H), 1.53 (s, 1H), 1.50 (s, 1H), 1.43–1.29 (m, 4H), 1.21–1.13 (m, 1H), 1.07 (t, J = 3.2 Hz, 1H), 1.05 (d, J = 4.0 Hz, 1H), 0.99 (d, J = 6.8 Hz, 3H), 0.91 (s, 3H), 0.86 (d, J = 7.2 Hz, 3H)·^{13}C NMR (101 MHz, $CDCl_3$) δ 174.15, 172.85, 157.57, 143.30, 141.58, 138.00, 134.40, 129.96, 128.71, 126.44, 121.84, 84.99, 75.98, 72.47, 71.79, 66.32, 63.27, 51.97, 50.94, 49.19, 43.87, 41.74, 41.51, 39.85, 38.11, 36.51, 35.98, 35.14, 32.55, 31.33, 31.05, 29.01, 28.33, 28.10, 26.17, 24.55, 20.41, 18.64, 13.49, 10.43. ESI: m/z 713 $[M + H]^+$, 735 $[M + Na]^+$. HRMS (EI) calcd. For $C_{42}H_{52}N_2O_6S$ $[M + H]^+$ 713.3625, found 713.3624.

Compound 8. Starting from compound 7, the general procedure previously described gave compound **8** that was purified by chromatography on silica gel with MPLC Isolera Biotage eluting with a gradient of EtOAc in CH_2Cl_2 0–5 %, and recovered as a white solid (0.233 g, 85 % of yield). ^{1}H NMR (600 MHz, CD_3OD, δ ppm, J Hz) δ 6.96 (s, 1H), 6.75 (d, J = 1.3 Hz, 1H), 6.67 (dd, J = 2.8, 1.4 Hz, 1H), 5.41–5.38 (m, 1H), 5.05 (d, J = 3.4 Hz, 2H), 4.84 (dd, J = 6.2, 2.4, Hz, 2H), 3.73 (qd, J = 7.1, 4.2 Hz, 2H), 3.69–3.60 (m, 2H), 3.47–3.40 (m, 1H), 3.27–3.22 (m, 1H), 2.96 (dd, J = 4.2, 2.4 Hz, 1H), 2.38–2.12 (m, 7H), 2.03 (s, 1H), 1.96–1.89 (m, 2H), 1.83–1.80 (m, 2H), 1.76–1.74 (m, 2H), 1.66 (s, 3H), 1.59–1.51 (m, 3H), 1.45 (q, J = 7.9 Hz, 1H), 1.25 (m, 6H), 1.05 (m, 2H), 1.01 (d, J = 6.7 Hz, 3H), 0.99 (s, 3H), 0.89 (m, 3H). ^{13}C NMR (151 MHz, CD_3OD, δ ppm) δ 157.96, 147.99, 143.15, 141.75, 140.57, 126.20, 124.77, 122.25, 121.27, 119.52, 110.38, 102.31, 85.31, 78.17, 75.89, 72.17, 71.07, 67.01, 62.93, 60.14, 59.02, 58.99, 56.95, 53.41, 52.01, 48.71, 42.05, 41.52, 41.16, 38.06, 36.33, 32.04, 30.66, 28.50, 28.03, 24.24, 19.47, 17.59, 13.59, 13.93, 12.36, 9.31. ESI: m/z 688 $[M + H]^+$, 710 $[M + Na]^+$. HRMS (EI) calcd. For $C_{41}H_{53}NO_8$ $[M + H]^+$ 688.3850, found 688.3848.

General procedure for CuCAAC reaction. Triazole 6. Product **4** (50 mg, 0.07 mmol) and the azide **5** (9 mg, 0.056 mmol) were dissolved in dry DMF (2 mL) under Ar. The solution was degassed with three cycles of Ar/vacuum. To this solution, a freshly prepared mixture of $Cu(OAc)_2$ (4 mg, 0.021 mmol) and Na ascorbate (8 mg, 0.042 mmol) in water (2 mL), degassed by Ar/vacuum cycles, was added dropwise. The reaction mixture was stirred under Ar at rt. for 16 h. The solvent was evaporated, and the crude purified by flash chromatography on silica gel eluting with a gradient of MeOH in CH_2Cl_2 0–10 % to give **6** as a white solid, 36 mg, 0.041 mmol, 74 % yield. ^{1}H NMR (600 MHz, $CDCl_3$, δ ppm, J Hz) δ 7.55 (s, 1H), 7.49 (d, J = 8.0 Hz, 2H), 7.31 (d, J = 8.0 Hz, 2H), 5.39 (s, 1H), 5.18–5.11 (m, 2H), 4.76 (s, 2H), 4.35 (t, J = 6.9 Hz, 2H), 4.11 (dd, J = 9.1, 4.1 Hz, 1H), 3.70–3.64 (m, 1H), 3.57 (ddd, J = 14.7, 10.8, 5.5 Hz, 2H), 3.26–3.16 (m, 2H), 2.98 (dd, J = 20.5, 8.5 Hz, 1H), 2.88–2.84 (m, 1H), 2.71 (dd, J = 18.7, 4.0 Hz, 1H), 2.37 (dd, J = 27.2, 9.6 Hz, 3H), 2.31–2.20 (m, 4H), 2.21–2.13 (m, 1H), 1.96–1.88 (m, 4H), 1.88–1.78 (m, 2H), 1.77–1.70 (m, 3H), 1.68 (s, 4H), 1.61–1.50 (m, 2H), 1.40–1.30 (m, 2H), 1.39–1.32 (m, 4H), 1.30 (s, 1H), 1.20 (t, J = 8.2 Hz, 1H), 1.14–1.07 (m, 2H), 1.03 (d, J = 6.8 Hz, 3H), 0.96 (s, 3H), 0.91 (d, J = 7.2 Hz, 3H). ^{13}C NMR (151 MHz, $CDCl_3$, δ ppm) δ 176.37, 175.12, 173.81, 157.65, 143.33, 141.60, 141.36, 137.67, 133.84, 130.62, 128.68, 126.45, 123.11, 121.86, 85.03, 72.48, 71.82, 66.44, 63.27,

52.00, 50.93, 49.99, 49.21, 43.91, 41.73, 41.59, 41.54, 38.13, 36.53, 36.07, 34.09, 33.30, 32.57, 31.32, 31.07, 29.67, 29.03, 28.34, 25.57, 24.57, 23.86, 20.47, 18.67, 13.51, 10.46. HRMS (EI) calcd. For $C_{48}H_{63}N_5O_8S$ $[M + H]^+$ 870.4476, found 870.4474.

Compound 9 Obtained as a white solid 41 mg, 0.048 mmol, 85 % yield. **^{1}H NMR** (600 MHz, $CDCl_3$, δ ppm, J Hz) δ 7.69 (s, 1H), 6.90 (s, 1H), 6.70 (s, 1H), 6.62 (s, 1H), 5.39–5.37 (m, 1H), 5.33 (s, 2H), 5.07–5.01 (m, 2H), 4.38 (t, J = 6.0 Hz, 2H), 3.76 (qd, J = 7.1, 2.1 Hz, 2H), 3.66 (dd, J = 13.0, 4.1 Hz, 1H), 3.56 (qd, J = 10.5, 4.5 Hz, 2H), 3.22 (dd, J = 10.3, 7.3 Hz, 1H), 2.98–2.91 (m, 1H), 2.87 (s, 1H), 2.38 (dd, J = 13.0, 2.8 Hz, 1H), 2.34 (t, J = 7.1 Hz, 2H), 2.23 (m, 4H), 2.15 (dd, J = 16.8, 11.0 Hz, 1H), 1.98–1.92 (m, 2H), 1.91–1.83 (m, 3H), 1.82–1.78 (m, 1H), 1.78–1.69 (m, 3H), 1.68 (s, 4H), 1.59–1.49 (m, 2H), 1.39 (t, J = 7.9 Hz 3H), 1.32 (dd, J = 11.0, 4.0 Hz, 1H), 1.29 (d, J = 2.8 Hz, 1H), 1.27 (m, 4H), 1.19 (td, J = 13.5, 3.2 Hz, 1H), 1.10 (td, J = 11.8, 8.7 Hz, 1H), 1.02 (d, J = 6.8 Hz, 3H), 0.94 (s, 3H), 0.90 (d, J = 7.2 Hz, 3H). ^{13}C NMR (151 MHz, $CDCl_3$, δ ppm) δ 176.57, 157.87, 147.48, 143.73, 143.29, 141.61, 141.33, 134.08, 130.95, 126.51, 122.93, 121.88, 110.03, 102.54, 85.01, 72.55, 71.83, 70.56, 67.19, 63.61, 63.27, 61.30, 59.72, 59.67, 52.00, 50.05, 49.22, 49.00, 41.73, 41.54, 38.14, 36.53, 33.29, 32.60, 31.33, 31.08, 29.74, 29.02, 28.37, 25.78, 24.58, 23.89, 20.43, 18.67, 14.84, 13.52, 10.47. ESI: m/z 845 $[M + H]^+$, 867 $[M + Na]^+$, 843 $[M\text{-}H]^-$. HRMS (EI) calcd. For $C_{47}H_{64}N_4O_{10}$ $[M + H]^+$ 845.4701, found 845.4703.

Dibenzylcyclooctine derivative 14. Compound **6** (50 mg, 0.058 mmol) was dissolved in dry CH_2Cl_2 (5 mL) at rt. under N_2. EDC·HCl (19 mg, 0.099 mmol) and NHS (11 mg, 0.099 mmol) were added, and the reaction mixture was stirred at rt. for 16 h. The mixture was concentred and quickly filtrated on a pad of silica gel using CH_2Cl_2: MeOH 6:1. The solution was concentred under reduced pressure and immediately used for the next step. The NHS-ester (21 mg, 0.022 mmol) was dissolved in dry DMF (280 mL) at rt. under N_2. Dibenzylcyclooctine amine **13** (6 mg, 0.020 mmol) and triethylamine (6 mL, 0.042 mmol) were added, and the reaction mixture stirred at rt. for 16 h. The solvent was evaporated under reduced pressure with addition of heptane, and the crude was purified by silica gel flash chromatography eluting with a gradient of MeOH in CH_2Cl_2 0–10 % to give compound **14** as a white solid (13 mg, 58 % yield). ^{1}H NMR (600 MHz, $CDCl_3$, δ ppm, J Hz) δ 7.69 (d, J = 7.6 Hz, 1H), 7.55 (d, J = 6.7 Hz, 1H), 7.49 (d, J = 8.1 Hz, 2H), 7.46–7.36 (m, 4H), 7.32 (m, 4H), 7.25 (d, J = 7.5 Hz, 1H), 6.05 (s, 1H), 5.38 (s, 1H), 5.16 (s, 1H), 5.13 (d, J = 5.6 Hz, 2H), 4.75 (d, J = 2.5 Hz, 2H), 4.31 (t, J = 7.2 Hz, 2H), 4.09 (dd, J = 9.1, 4.1 Hz, 1H), 3.73–3.64 (m, 2H), 3.60–3.47 (m, 2H), 3.37–3.31 (m, 1H), 3.26–3.20 (m, 2H), 3.20–3.13 (m, 1H), 3.00–2.90 (m, 1H), 2.88–2.83 (m, 1H), 2.70 (dd, J = 18.7, 4.2 Hz, 1H), 2.46 (ddd, J = 16.6, 7.5, 3.8 Hz, 1H), 2.42–2.35 (m, 1H), 2.27–2.20 (m, 3H), 2.19 (s, 1H), 2.01–1.94 (m, 3H), 1.94–1.79 (m, 6H), 1.71 (s, 1H), 1.68 (s, 3H), 1.55 (dd, J = 15.3, 7.5 Hz, 3H), 1.44–1.38 (m, 2H), 1.37–1.31 (m, 2H), 1.30–1.24 (m, 4H), 1.24–1.15 (m, 2H), 1.14–1.05 (m, 2H), 1.02 (d, J = 6.8 Hz, 3H), 0.94 (s, 3H), 0.90 (d, J = 7.3 Hz, 3H). ^{13}C NMR (151 MHz, $CDCl_3$, δ ppm) δ 174.94, 173.62, 172.30, 172.22, 157.62, 151.01, 148.01, 143.31, 141.68, 141.40, 137.64, 133.77, 133.74, 132.11, 130.76, 129.54, 129.05, 128.69, 128.49, 128.36, 127.89, 127.28, 126.48, 125.55, 123.00, 122.92, 122.47, 121.81, 114.74, 107.82, 85.00, 74.08, 72.50, 71.75, 66.40, 63.30, 55.54, 52.01, 50.12, 49.22, 43.91, 41.78, 41.60, 41.54, 39.90, 38.15, 36.54, 36.07, 35.15, 34.83, 34.14, 32.59, 31.37, 31.08, 29.96, 29.04, 28.36, 26.00, 24.70, 24.59, 20.46, 18.68, 13.53, 10.47. ESI: m/z 1128 $[M + H]^+$. HRMS (EI) calcd. For $C_{66}H_{77}N_7O_8S$ $[M + H]^+$ 1128.5633, found 1128.5632.

Preparation of ADC 11. To a 10 mM DMSO solution of compound **9**, an aqueous solution of sulfo-NHS (2 eq, 100 mM) and an aqueous solution of EDC•HCl (2 eq, 100 mM) were added, and the mixture was stirred at room temperature for 16 h. Subsequently, 250 μL of cetuximab (0.025 eq, 10 mg/mL, EPPS pH 8.0) were added, and the mixture was gently mixed at room temperature for 1 h. An aqueous solution of glycine (2 eq, 40 mM) was added to quench the unreacted linker-payload system, and the mixture was incubated at room temperature for 10 min. The resulting bioconjugate was purified using Cytiva PD SpinTrap G25 5 K MWCO size-exclusion desalting columns as described by the manufacturer.

Pre-functionalization of Cetuximab. To 400 μL of Cetuximab (0.05 eq, 10 mg/mL, PBS pH 7.4) was added a 10 mM solution in DMSO of 14-azido-3,6,9,12-tetraoxatetradecanoic acid (**15**). The mixture was stirred at room temperature for 1 h. An aqueous solution of glycine (2 eq, 40 mM) was added to quench the unreacted linker-payload system, and the mixture was incubated at room temperature for 10 min. The resulting bioconjugate (**Ctx—N_3**) was purified as described above.

Preparation of ADC 16. To 450 μL of the functionalized Cetuximab (5.7 mg/mL in water) was added a DMSO solution of the linker-payload system (**14**, 80 eq), and the mixture was gently mixed at 4 °C for 16 h. The resulting bioconjugate was purified as described above.

Cell viability assay. 1,5 × 10^3/well A375 and 3 × 10^3/well SK-MEL-5 melanoma cells were seeded in triplicate in 96-well plates (Corning) with complete DMEM medium. After 24 h cells were treated in 2.5 % FBS DMEM with Cetuximab, Cyclopamine (**1**), unconjugated linker-payload system **9** and **4** and ADCs **11** and **16** at two different concentrations (100 μg/mL, 200 μg/mL) to compare the effect of ADCs with the single components. After 72 h of treatment the culture medium was removed, cells were fixed in paraformaldehyde (Kaltek Srl) for 10 min and then stained with Crystal Violet (Sigma- Aldrich) (0.1 % Crystal Violet, 20 % Methanol, dH_2O) for 15 min in mild agitation. After 24 h, cells were bleached with 10 % glacial acetic acid RPE (Carlo Erba) for 15 min in mild agitation, then the absorbance, which is proportional to the number of viable cells within every well, was measured at 595 nm with VICTOR X5 (Multilabel Plate Reader, PerkinElmer).

Protein extraction and Western blot. Cells were lysed in cold RIPA buffer (50 mM Tris-HCl pH 7.5, 1 % NP-40, 150 mM NaCl, 5 mM EDTA, 0.25 % NaDOC, and 0.1 % SDS) supplemented with protease and phosphatase inhibitors and centrifuged at 20,000 ×g for 20 min at 4 °C. Supernatant was collected as whole cell extract (WCE). Equal amounts of protein were resolved by SDS-polyacrylamide gel electrophoresis, transferred onto nitrocellulose membranes, and incubated for 1 h in blocking buffer at room temperature. Primary antibodies are reported in Supplementary Table S2. Blotted membranes were developed by using SuperSignal West Femto (Thermo Fisher Scientific) and imaged with ChemiDoc Imaging Systems (Bio-Rad).

Cytofluorimetric analysis of cell cycle. A375 and SK-MEL-5 cells were seeded in 6-multiwell plates (Corning) in complete medium and treated after 24 h in 2.5 % FBS medium with Cetuximab, **1**, **9** and ADC **11** at 200 μg/mL concentration. After 72 h cells were collected and fixed in cold 70 % ethanol. Cells were stained with a solution of Ribonuclease (RNase) 50 U/mL and Propidium Iodide 50 μg/mL for 20 min in the dark. Flow cytometry analysis was performed using CytoFLEX S (BD Beckman Coulter).

Cytofluorimetric analysis of cell apoptosis. Cellular apoptosis was analyzed using the Annexin V/7-Aminoactinomycin D (7-AAD) apoptosis detection kit (BD PharmingenTM). A375 and SK-MEL-5 melanoma cells were seeded in 6-multiwell plates (Corning) in complete medium and after 24 h were treated with Cetuximab, Cyclopamine (**1**), unconjugated payload (**9**) and ADC **11** at 200 μg/mL concentration. After 72 h of treatment, cells were collected and resuspended in 50 μL of Binding Buffer (BD PharmingenTM). Cells were stained with Annexin V/7-AAD and analyzed by flow cytometry using CytoFLEX S (BD Beckman Coulter).

Antibody internalisation assay. For antibody internalisation, we used the IncuCyte® FabFluor-pH Red Antibody Labeling (Sartorius). 3 × 10^3/well A375 and 5 × 10^3/well SK-MEL-5 cells were seeded (50 μL) into a 96-well plate. After 24 h, antibody tests (Cetuximab and ADC **11**) were mixed with FabFluor Reagent at a molar ratio of 1:3 in media; culture medium was used as negative control. The intensity of the FabFluor reagent is pH dependent. As such, a fluorogenic signal is observed as the Fab-Ab complex is internalized and processed via acidic

lysosomes and endosomes. Ab-Fab mixes were added to cells according to manufacturer's instructions, and live cells were visually identified at 20× and 40× magnification with Nikon Eclipse TE300 microscope (Nikon Instruments Inc.) equipped with a Photometrics CoolSNAP CF camera (Teledyne Photometrics, Tucson AZ). Cells were imaged in contrast-phase brightfield illumination and fluorescence images were collected using the following filter block system: excitation filter 510–560 nm, dichroic filter 575 nm and emission filter 590 nm. Red fluorescence channels were acquired after 48 h from addition of Ab-Fab mix to cells.

MT and EP conceptualised the project. GR, FM, DZ, GI, LM, AM and ECr performed experiments and conducted data interpretation. MT, EP, EC and BS supervised the project. The manuscript was written with input from all authors.

FM and ECr acknowledge a studentship from AIRC (under IG 2017 – ID. 20758 project). LM was supported by a post-doctoral fellowship from AIRC (project n. 30051). BS was supported by an AIRC grant (IG 23091). EP acknowledges the financial support from the PNRR Tuscany Health Ecosystem–Ecosistemi dell'innovazione CUP B83C22003930001 –ECS_00000017–Precision Medicine & Personalized Healthcare.

CRediT authorship contribution statement

Giovanni Ricciardella: Methodology, Investigation. **Francesca Migliorini:** Methodology, Investigation. **Luisa Maresca:** Methodology, Investigation. **Elena Cini:** Supervision. **Giovanni Ievoli:** Methodology, Investigation. **Elena Petricci:** Supervision, Conceptualization. **Maurizio Taddei:** Conceptualization. **Demetra Zambardino:** Methodology. **Barbara Stecca:** Supervision. **Alberto Montalbano:** Methodology. **Enrica Crivaro:** Methodology, Investigation.

Declaration of competing interest

The authors declare the following financial interests/personal relationships which may be considered as potential competing interests: Maurizio Taddei reports financial support was provided by AIRC Foundation for Cancer Research. If there are other authors, they declare that they have no known competing financial interests or personal relationships that could have appeared to influence the work reported in this paper.

Appendix A. Supplementary data

Supplementary data to this article can be found online at https://doi.org/10.1016/j.bioorg.2025.109452.

Data availability

Data will be made available on request.

References

[1] R.F. Keeler, Teratogenic compounds of Veratrum californicum. IV. First isolation of veratramine and alkaloid Q and a reliable method for isolation of cyclopamine, Phytochemistry (Elsevier) 7 (1968) 303.
[2] R.F. Keeler, W. Binns, Teratogenic compounds of Veratrum californicum (Durand). V. Comparison of cyclopian effects of steroidal alkaloids from the plant and structurally related compounds from other sources, Teratology 1 (1968) 5–10, https://doi.org/10.1002/tera.1420010103.
[3] L.F. James, K.E. Panter, W. Gaffield, R.J. Molyneux, Biomedical applications of poisonous plant research, J. Agric. Food Chem. 52 (2004) 3211–3230, https://doi.org/10.1021/jf0308206.
[4] B. Thazhackavayal Baby, A.M. Kulkarni, P.K.R. Gayam, K.B. Harikumar, J. M. Aranjani, Beyond cyclopamine: targeting hedgehog signaling for cancer intervention, Arch. Biochem. Biophys. 754 (2024) 109952, https://doi.org/10.1016/j.abb.2024.109952.
[5] S. Pietrobono, S. Gagliardi, B. Stecca, Non-canonical hedgehog Signaling pathway in Cancer: activation of GLI transcription factors beyond smoothened, Front. Genet. 10 (2019) 556, https://doi.org/10.3389/fgene.2019.00556.
[6] J.K. Chen, J. Taipale, M.K. Cooper, P.A. Beachy, Inhibition of hedgehog signaling by direct binding of cyclopamine to smoothened, Genes Dev. 16 (2002) 2743–2748, https://doi.org/10.1101/gad.1025302.
[7] J.K. Chen, J. Taipale, K.E. Young, T. Maiti, P.A. Beachy, Small molecule modulation of smoothened activity, Proc. Nat. Acad. Sci. U S A 99 (2002) 14071–14076, https://doi.org/10.1073/pnas.182542899.
[8] R.F. Keeler, Teratogenic compounds in Veratrum californicum (Durand) IX. Structure-activity relation, Teratology 3 (1970) 169–174.
[9] R.F. Keeler, Teratogenic compounds in Veratrum californicum (Durand) X. Cyclopia in rap pits produced by cyclopamine, Teratology 3 (1970) 175–180.
[10] M.R. Tremblay, M. Nevalainen, S.J. Nair, J.R. Porter, A.C. Castro, M.L. Behnke, L.-C. Yu, M. Hagel, K. White, K. Faia, L. Grenier, M.J. Campbell, J. Cushing, C. N. Woodward, J. Hoyt, M.A. Foley, M.A. Read, J.R. Sydor, J.K. Tong, V. J. Palombella, K. McGovern, J. Adams, Semisynthetic Cyclopamine analogues as potent and orally bioavailable hedgehog pathway antagonists, J. Med. Chem. 51 (2008) 6646–6649, https://doi.org/10.1021/jm8008508.
[11] T. Cosio, M. Di Prete, C. Di Raimondo, V. Garofalo, F. Lozzi, C. Lanna, E. Dika, A. Orlandi, M.C. Rapanotti, L. Bianchi, E. Campione, Patidegib in dermatology: a current review, Int. J. Mol. Sci. 22 (2021) 10725, https://doi.org/10.3390/ijms221910725.
[12] J.T. Lear, L.M. Morris, D.B. Ness, L.D. Lewis, Pharmacokinetics and pharmacodynamics of hedgehog pathway inhibitors used in the treatment of advanced or treatment-refractory basal cell carcinoma, Expert. Rev. Clin. Pharmacol. 16 (2023) 1211–1220, https://doi.org/10.1080/17512433.2023.2285849.
[13] E. Callegari, S. Tse, A.C. Doran, T.C. Goosen, N. Shaik, Physiologically based pharmacokinetic Modeling of the drug-drug interaction between CYP3A4 substrate Glasdegib and moderate CYP3A4 inducers in lieu of a clinical study, J. Clin. Pharmacol. 64 (2024) 80–93, https://doi.org/10.1002/jcph.2348.
[14] A.D. Hobson, The medicinal chemistry evolution of antibody–drug conjugates, RSC Med. Chem. 15 (2024) 809–831, https://doi.org/10.1039/D3MD00674C.
[15] K. Liu, M. Li, Y. Li, Y. Li, Z. Chen, Y. Tang, M. Yang, G. Deng, H. Liu, A review of the clinical efficacy of FDA-approved antibody–drug conjugates in human cancers, Mol. Cancer 23 (2024) 62, https://doi.org/10.1186/s12943-024-01963-7.
[16] N. Lu, J. Wu, M. Tian, S. Zhang, Z. Li, L. Shi, Comprehensive review on the elaboration of payloads derived from natural products for antibody-drug conjugates, Eur. J. Med. Chem. 268 (2024) 116233, https://doi.org/10.1016/j.ejmech.2024.116233.
[17] L. Conilh, L. Sadilkova, W. Viricel, C. Dumontet, Payload diversification: a key step in the development of antibody–drug conjugates, J. Hematol. Oncol. 16 (2023) 3, https://doi.org/10.1186/s13045-022-01397-y.
[18] E. Cini, V. Faltoni, E. Petricci, M. Taddei, L. Salvini, G. Giannini, L. Vesci, F. M. Milazzo, A.M. Anastasi, G. Battistuzzi, R. De Santis, Antibody drug conjugates (ADCs) charged with HDAC inhibitor for targeted epigenetic modulation, Chem. Sci. 9 (2018) 6490–6496, https://doi.org/10.1039/C7SC05266A.
[19] L. Vesci, E. Bernasconi, F.M. Milazzo, R. De Santis, E. Gaudio, I. Kwee, A. Rinaldi, S. Pace, V. Carollo, G. Giannini, F. Bertoni, Preclinical antitumor activity of ST7612AA1: a new oral thiol-based histone deacetylase (HDAC) inhibitor, Oncotarget 6 (2015) 5735–5748, https://doi.org/10.18632/oncotarget.3240.
[20] F.M. Milazzo, L. Vesci, A.M. Anastasi, C. Chiapparino, A. Rosi, G. Giannini, M. Taddei, E. Cini, V. Faltoni, E. Petricci, V. Carollo, R. De Santis, ErbB2 targeted epigenetic modulation: anti-tumor efficacy of the ADC trastuzumab-HDACi ST8176AA1, Front. Oncol. 9 (2020), https://doi.org/10.3389/fonc.2019.01534.
[21] C. Cianferotti, V. Faltoni, E. Cini, E. Ermini, F. Migliorini, E. Petricci, M. Taddei, L. Salvini, G. Battistuzzi, F.M. Milazzo, R. De Santis, G. Giannini, Antibody drug conjugates with hydroxamic acid cargos for histone deacetylase (HDAC) inhibition, Chem. Commun. 57 (2021) 867–870, https://doi.org/10.1039/d0cc06131j.
[22] A. Giannis, P. Heretsch, V. Sarli, A. Stößel, Synthesis of Cyclopamine using a biomimetic and diastereoselective approach, Angew. Chem. Int. Ed. 48 (2009) 7911–7914, https://doi.org/10.1002/anie.200902520.
[23] M. Sofiadis, D. Xu, A.J. Rodriguez, B. Nissl, S. Clementson, N.N. Petersen, P. S. Baran, Convergent Total synthesis of (−)-Cyclopamine, J. Am. Chem. Soc. 145 (2023) 21760–21765, https://doi.org/10.1021/jacs.3c09085.
[24] M.W. Turner, R. Cruz, J. Mattos, N. Baughman, J. Elwell, J. Fothergill, A. Nielsen, J. Brookhouse, A. Bartlett, P. Malek, X. Pu, M.D. King, O.M. McDougal, Cyclopamine bioactivity by extraction method from Veratrum californicum, Bioorg. Med. Chem. 24 (2016) 3752–3757, https://doi.org/10.1016/j.bmc.2016.06.017.
[25] A. Zuo, D. He, C. Sun, Y. Wen, H. Li, C. Kou, G. Shao, Z. Xue, R. Ma, J. Wei, J. Liu, P. Ma, Integration of induction, system optimization and genetic transformation in Veratrum californicum var. vitro cultures to enhance the production of cyclopamine and veratramine, Plant Physiol. Biochem. 216 (2024) 109087, https://doi.org/10.1016/j.plaphy.2024.109087.
[26] P.H. Winegar, G.A. Hudson, L.B. Dell, M.C.T. Astolfi, J. Reed, R.D. Payet, H.C. J. Ombredane, A.T. Iavarone, Y. Chen, J.W. Gin, C.J. Petzold, A.E. Osbourn, J. D. Keasling, Verazine biosynthesis from simple sugars in engineered Saccharomyces cerevisiae, Metab. Eng. 85 (2024) 145–158, https://doi.org/10.1016/j.ymben.2024.07.011.
[27] W. Hou, H. Lin, Y. Wu, C. Li, J. Chen, X.-Y. Liu, Y. Qin, Divergent and gram-scale syntheses of (−)-veratramine and (−)-cyclopamine, Nat. Commun. 15 (2024) 5332, https://doi.org/10.1038/s41467-024-49748-2.
[28] F. Migliorini, E. Cini, E. Dreassi, F. Finetti, G. Ievoli, G. Macrì, E. Petricci, E. Rango, L. Trabalzini, M. Taddei, A pH-responsive crosslinker platform for antibody-drug conjugate (ADC) targeting delivery, Chem. Commun. 58 (2022) 10532–10535, https://doi.org/10.1039/d2cc03052g.

[29] L. Angiolini, F. Manetti, O. Spiga, A. Tafi, A. Visibelli, E. Petricci, Machine learning for predicting the drug-to-antibody ratio (DAR) in the synthesis of antibody–drug conjugates (ADCs), J. Chem. Inf. Model. 65 (2025) 5847–5855, https://doi.org/10.1021/acs.jcim.5c00037.

[30] W. Shalata, Z.G. Attal, A. Solomon, S. Shalata, O. Abu Saleh, L. Tourkey, F. Abu Salamah, I. Alatawneh, A. Yakobson, Melanoma management: exploring staging, prognosis, and treatment innovations, Int. J. Mol. Sci. 25 (2024), https://doi.org/10.3390/ijms25115794.

[31] S. Pietrobono, E. Gaudio, S. Gagliardi, M. Zitani, L. Carrassa, F. Migliorini, E. Petricci, F. Manetti, N. Makukhin, A.G. Bond, B.D. Paradise, A. Ciulli, M. E. Fernandez-Zapico, F. Bertoni, B. Stecca, Targeting non-canonical activation of GLI1 by the SOX2-BRD4 transcriptional complex improves the efficacy of HEDGEHOG pathway inhibition in melanoma, Oncogene 40 (2021) 3799–3814, https://doi.org/10.1038/s41388-021-01783-9.

[32] Z. Taha, M.J.F. Crupi, N. Alluqmani, F. Fareez, K. Ng, J. Sobh, E. Lee, A. Chen, M. Thomson, M.M. Spinelli, C.S. Ilkow, J.C. Bell, R. Arulanandam, J.-S. Diallo, Syngeneic mouse model of human HER2+ metastatic breast cancer for the evaluation of trastuzumab emtansine combined with oncolytic rhabdovirus, Front. Immunol. 14 (2023), https://doi.org/10.3389/fimmu.2023.1181014.

[33] S.R. Wilson, M.F. Strand, A. Krapp, F. Rise, D. Petersen, S. Krauss, Hedgehog antagonist cyclopamine isomerizes to less potent forms when acidified, J. Pharm. Biomed. Anal. 52 (2010) 707–713, https://doi.org/10.1016/J.JPBA.2010.02.017.

[34] W. Armarego, C. Chai, Purification of Organic Chemicals, Purification of Laboratory Chemicals, Seventh edition, 2013, pp. 103–554, https://doi.org/10.1016/B978-075067571-0/50008-9.

[35] Y. Wu, T. Wang, D.Y.W. Ng, T. Weil, Multifunctional polypeptide-PEO nanoreactors via the hydrophobic switch, Macromol. Rapid Commun. 33 (2012) 1474, https://doi.org/10.1002/marc.201200227.